Abstract for the 29th Intl Workshop on Water Waves and Floating Bodies, Osaka (Japan), March 30 – April 02, 2014

Study on Slamming and Whipping Response of Ship Structure

by Jung-Hyun Kim[1*], Yonghwan Kim[1], Alexander A. Korobkin[2] , Dong-Yeon Lee[3]

[1]Dept. of Naval Architecture and Ocean Engineering, Seoul National University, Seoul, Korea
[2]School of Mathematics, University of East Anglia, Norwith, UK
[3]Samsung Ship Model Basin, Samsung Heavy Industries, Daejeon, Korea
E-mail: *yhwankim@snu.ac.kr*

Highlights:

- Ship structural hydroelasticity is observed in the presence of slamming loads and whipping responses.
- GWM shows a fair performance in the wedge drop test with similar results in peak pressure, pressure descent, and forces to those of the experiment. Peak pressure is mainly proportional to a square of velocity, while pressure descent is proportional to acceleration.
- Fully-coupled hydroelastic analysis of whipping response via GWM shows a good correspondance with measurements of the segmented ship model test.

1. Introduction

Whipping is a critical problem in ship structural design and operation strategy. It is obvious that whipping acts to increase ultimate and fatigue strength criteria and to reduce ship forward speed in severe sea states. This study aims to compute slamming loads and whipping responses by a numerical method. In order to predict whipping by the numerical method, we should calculate slamming load in an accurate manner and solve the fluid-structure interaction problem. An analytic approach for the evaluation of slamming load was pioneered by von Karman(1929) and Wagner(1932). Wagner's approach was modified to take into account the exact body boundary and to apply the leading-order free surface boundary condition up to the instantaneous intersection between body and free surface (e.g. Zhao and Faltinsen [1]). The present analysis for slamming load is based on this generalized Wagner model (GWM).

The other part of the numerical method is to solve the fluid-structure interaction problem which computes flexible structural motion of ship structure in the presence of ocean waves. In this study, a 3-D Rankine panel method, strongly coupled with 1-D and 3-D finite element method (FEM), is used in time domain. This method was successfully applied to springing problems by Kim *et al*. [2]. A similar approach using Green functions was applied to springing and whipping problems by Malenica and Tuitman [3], but the present study is based on a complete time-domain approach which solves the springing and whipping simultaneously with both direct time integration and modal method.

In this abstract, firstly, the numerical method to predict slamming loads and whipping responses is briefly described. Then, GWM is validated against the wedge drop test by a thorough comparison of pressure and force signals. Finally, the computational result of whipping is compared with an experimental result in terms of measured vertical bending moments and pressures. In addition, the characteristics of whipping in a regular wave are investigated by the decomposition of high frequency oscillation and the comparison of slamming modal forces.

2. A Fully-Coupled Hydroelastic Analysis Method

A fully-coupled approach is essential for numerical hydroelastic analysis on springing and whipping of ship structure. In this study, the interaction problem between fluid and structure is solved by coupling a 3-D Rankine panel method for hydrodynamic field, 1-D and 3-D FEM for ship structure and GWM for slamming load analysis. In the 3-D Rankine panel method, the velocity potential ϕ in fluid domain Ω_F is decomposed into the basis potential Φ, the incident potential ϕ_I, and the disturbed potential ϕ_d. The basis potential corresponds to the velocity potential of a double body. The free surface elevation ζ, can also be decomposed into incident elevation ζ_I, and disturbed elevation ζ_d .The decomposed potentials can be uniquely determined by boundary conditions as follows: kinematic and dynamic free-surface boundary conditions; body boundary condition; and radiation condition. Kinematic and dynamic free-surface boundary conditions are linearized on the still water level, $z = 0$, as follows:

$$\frac{\partial \zeta_d}{\partial t} - (\vec{U} - \nabla\Phi)\cdot\nabla\zeta_d = \frac{\partial^2\Phi}{\partial z^2}\zeta_d + \frac{\partial \phi_d}{\partial z} + (\vec{U} - \nabla\Phi)\cdot\nabla\zeta_I \quad \text{on z = 0} \tag{1}$$

$$\frac{\partial \phi_d}{\partial t} - (\vec{U} - \nabla\Phi)\cdot\nabla\phi_d = -\frac{\partial\Phi}{\partial t} - g\zeta_d + \left[\vec{U}\cdot\nabla\Phi - \frac{1}{2}\nabla\Phi\cdot\nabla\Phi\right] + (\vec{U} - \nabla\Phi)\cdot\nabla\phi_I \quad \text{on z = 0} \tag{2}$$

where $\vec{U}$ denotes the forward speed vector of the ship. The body boundary condition is linearized on the mean body surface, $\bar{S}_B$, as

$$\frac{\partial \phi_d}{\partial n} = \left[(\vec{\delta}\cdot\nabla)(\vec{U} - \nabla\Phi) + ((\vec{U} - \nabla\Phi)\cdot\nabla)\vec{\delta}\right]\cdot\vec{n} + \frac{\partial\vec{\delta}}{\partial t}\cdot\vec{n} - \frac{\partial\phi_I}{\partial n} \quad \text{on } \bar{S}_B \tag{3}$$

where $\vec{\delta}$ and $\vec{n}$ are the displacement vector and the normal vector on the body surface, respectively. Through this linearization, the terms up to order of ε remain. It should be noted that the displacement of body should be defined locally since the body is flexible. Therefore, $\vec{\delta}$ should be defined locally. Such kind of technical issues were explained by Kim and Kim [4].

The initial value problem of GWM in an x-y plane is expressed as follows:

$$\nabla^2 \varphi = 0 \tag{4}$$

$$\varphi = 0 \qquad (y = H(t)) \tag{5}$$

$$S(x,t) = \varphi_y(x, H(t), t) \qquad (|x| > c(t)) \tag{6}$$

$$\varphi_y = f'(x)\varphi_x - \dot{h}(t) \qquad (y = f(x) - h(t),\ |x| < c(t)) \tag{7}$$

$$\varphi \to 0 \qquad (x^2 + y^2 \to \infty) \tag{8}$$

$$H(t) = f(c(t)) - h(t) \tag{9}$$

$$S(x,0) = 0, \quad c(0) = 0 \tag{10}$$

where φ is the velocity potential, $H(t)$ is the y-coordinate at the contact due to the splash-up of the free surface, $S(x,t)$ is the vertical velocity of the free surface, $f'(x)$ is the slope of the body geometry, $\dot{h}(t)$ is the water entry velocity of the body, $c(t)$ is the x-coordinate at the contact. The initial boundary value problem can be solved using a conformal mapping. The final form of pressure distribution is expressed as follows:

$$p = \rho \dot{h}^2 P_v(\xi, c) + \rho \ddot{h} P_w(\xi, c) \tag{11}$$

$$P_v(\xi,c) = \frac{X_c(\xi,c)}{N(c)} \frac{\xi}{S(\xi,c)} (1-\xi)^{-k(c)} - \frac{0.5}{1+f_x^2(X)} \frac{\xi^2}{S^2(\xi,c)} (1-\xi)^{-2k(c)} + \frac{F'_\infty(c)}{N(c)} \sqrt{1-\xi^2} + \frac{1}{2} - \frac{f_x(c)}{N(c)} \tag{12}$$

$$P_w(\xi,c) = f(X) - f(c) + F_\infty(c)\sqrt{1-\xi^2} \tag{13}$$

where ρ is the water density, ξ is the x-coordinates on the wetted body surface normalized by c, $F_\infty(c)$ is the coefficient in the far field asymptotic of the conformal mapping, and $N(c), f(X)$ and $f(c)$ are the functions from Wagner equation. The details about this part was introduced by Korobkin [5].

The final form explicitly guarantees that hydrodynamic pressure is not dependent on the time history of body motion but on the instantaneous velocity and acceleration. Thus, if the pressure distribution is solved with the zero initial condition which means that the body starts to enter the water from non-submerged condition, it can be used to other water entry problems with non-zero initial conditions. It can be achieved by setting offset values at the splash-up of free surface.

The pressures obtained by using the 3-D Rankine panel method and GWM are plugged into the equation of motion as external forces on ship. In the case of coupling with the 1-D FEM based on Timoshenko/Vlasov beam theory, the equation of motion is established using nodal motions in Cartesian coordinate system. The pressure is distributed to the adjacent nodes as nodal forces using weight factors which are obtained according to relative distance. The equation of flexible body motion can be integrated in time either using a direct manner or using modal superposition after eigenvalue analysis. On the other hand, when the 3-D FEM is coupled with the fluid solver, the equation of motion is established using modal motions in a generalized coordinate system based on eigenvectors. Eigenvectors on the collocation points of the 3-D Rankine panel method and GWM are recalculated using the linear interpolation of the eigenvalue analysis result of the 3-D FE model. Once the eigenvector is obtained, it is not necessary to use the 3-D FE solver the coupled analysis anymore. Fig. 1 shows the examples of hydrodynamic and structural meshes. The details about variable exchanges between the fluid and structural models were explained in the work of Kim et al. [6].

3. Wedge Drop Test: Comparison between GWM and Experiment

A series of drop tests with a symmetric wedge was carried out by MOERI/KIOST as part of WILS 3 JIP. The length, height and dead-rise angle of the wedge are 600 mm, 173 mm, and 30 degrees, respectively. In order to suppress the 3-D effect, the thickness of the wedge was determined to be 800mm, and a water blocking panel was attached to one end of the wedge. Pressure sensors were installed on the body surface, 50mm from the center line of the surface. Also a force sensor was also installed for the tests. The wedge was released from a drop height of 0.5 m from the water level. The acceleration of the wedge was measured by an accelerometer, and the displacement and velocity of the body were obtained by integrating the measured acceleration. The time history of the motion is applied as an input of the numerical simulation using GWM of the present study.

A static pressure is added to the dynamic pressure in equation (11) prior to comparison with the measured pressure. Fig. 2 shows the comparison of pressure and force signals between computation and experiment. The computational result shows a very similar signal with that of the experimental result. The peak value is fully proportional to the square of velocity, whereas pressure descent is significantly affected by the component proportional to acceleration. It is observed that the computation tends to overestimate the pressure after 1.08 sec. In the assumption of GWM, the gravity term is neglected from the dynamic free surface condition because $gT/V \ll 1$ is assumed where T is the duration of water entry, and V is the velocity of water entry. However, this assumption is not valid after 1.08sec; therefore, it is a reasonable result. In the force comparison, almost the same tendency with that of pressure between computational and experimental results is observed. It may imply that pressure distribution is similar between the computation and experiment. The overall tendency observed in the present study shows that GWM provides very good agreement of pressure and force signals with the experiment in the early stage of water-entry impact.

4. Computation of Whipping and Segmented Model Test

The segmented model test of an 18,000 TEU containership is carried out in Samsung Ship Model Basin (SSBM) as a part of ONR Project. Fig. 3 shows the segmented model of 1/60 scale and the installation of pressure sensors in bow area. Computation is performed using the fully-coupled method of 1-D FEM in conjunction with GWM. The details of the experimental and computational models can be found in the work of Kim et al. [6].

Fig. 4(a) compares whipping-dominant response and pressure in a regular wave condition of 14-sec period between computation and experiment. Overall, the computational results show similar whipping response with experiment. By conducting additional computation without slamming loads and flexibility, whipping and springing components can be separated from the total vertical bending moment. In this case, it can be seen that high-frequency oscillation is mainly induced by bow-flare slamming and reduced by stern slamming and springing.(see Fig. 4(b))

Pressure sensors are installed at two different heights of the section of 0.025Lbp from FP - one at 5.5m and another at 10.5m above the calm water level in full scale. Fig. 4(c) and (d) compare the pressure signals of these two locations. As shown in the figures below, two sensors obtain different shapes in pressure signals. For the first sensor P1 at 10.5m from waterline, dynamic component of pressure is dominant and its shape is very sharp. However, static component of pressure is dominant and the shape of dynamic component is not sharp for the second sensor P2 at 5.5m from waterline.

It should be mentioned that the peaks of slamming pressure are not regularly repeated although incident waves are regular. Therefore, the measured magnitudes vary significantly. Fig. 4(c) and 4(d) are the examples which show good agreement between computation and experiment. The detailed observation and comparison will be shown later.

5. Some Findings

Some key findings from this study are as follows:

- In the wedge drop test, GWM shows a very good agreement in pressure and force signals with experiment in early water-entry stage. Peak pressure is mainly proportional to the square of velocity, and pressure descent is proportional to acceleration.
- The fully-coupled numerical model in conjunction with GWM simulates high-frequency oscillations similar to those of the model test. Total high-frequency oscillation due to ship structural hydroelasticity is a mixture of super harmonic springing and whipping due to bow flare and stern slamming.
- Total pressure signals near FP show a good agreement between computational and model test. Dynamic component is dominant and its shape is very sharp in the upper sensor, whereas static component is dominant in the sensor installed at a lower position, nearer to still-water level.

Acknowledgements

This study has been carried out as a part of a project funded by LRF*[1]-Funded Research Center at Seoul National University for Fluid-Structure Interaction, and NICOP (N11-57) by ONR. Their supports are greatly appreciated.
(*[1]LRF: The Lloyd's Register Foundation).

References

[1] Zhao, R. and Faltinsen, O.M. 1993, Water entry of two-dimensional bodies, *Journal of Fluid Mechanics*, 246 pp.593-612.

[2] Kim, J.H., Kim, K.H., Jung, B.H., Choi, J.H., and Kim, Y. 2012, Analysis on Ship Springing Using Fully-Coupled FSI Models, *In: Proceedings of the 6th International Conference on Hydroelasticity in Marine Technology*, Tokyo, Japan.

[3] Malenica, S. and Tuitman, J.T. 2008, 3DFEM-3DBEM Model for Springing and Whipping Analysis of Ships, *In: Proceedings of the International Conference on Design and Operation of Containerships*, London, UK

[4] Kim, K.H. and Kim, Y. 2008, On Technical Issues in the Analysis of Nonlinear Ship Motion and Structural Loads in Waves by a Time-Domain Rankine Panel Method, *IWWWFB23*, Jeju, Korea

[5] Korobkin, A.A. 2011, Semi-analytical approach in Generalized Wagner Model, *IWWWFB26*, Athens, Greece.
[6] Kim, J.H., Kim, K.H., Lee, D.Y., Jung, B.H. and Kim, Y. 2013, A Fully Coupled BEM-FEM Analysis on Ship Structural Hydroelasticity and Experimental Validation, *In: Proceeding of the 12th International Symposium on Practical Design of Ships and Other Floating Structures*, PRADS2013, Changwon, Korea.

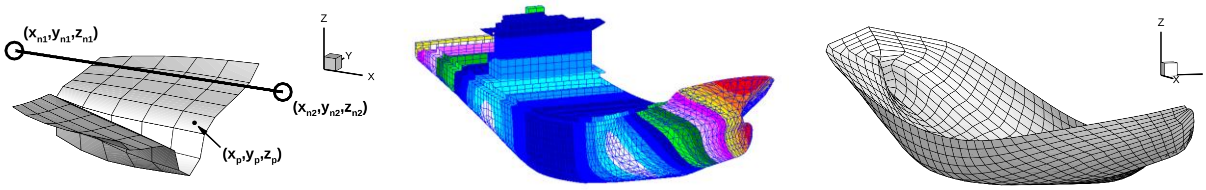

Fig. 1 Hydrodynamic and structural meshes (left: panel meshes and two adjacent nodes in 1-D FEM, middle: original eigenvector of 3-D FEM, right: recalculated eigenvector on panel meshes)

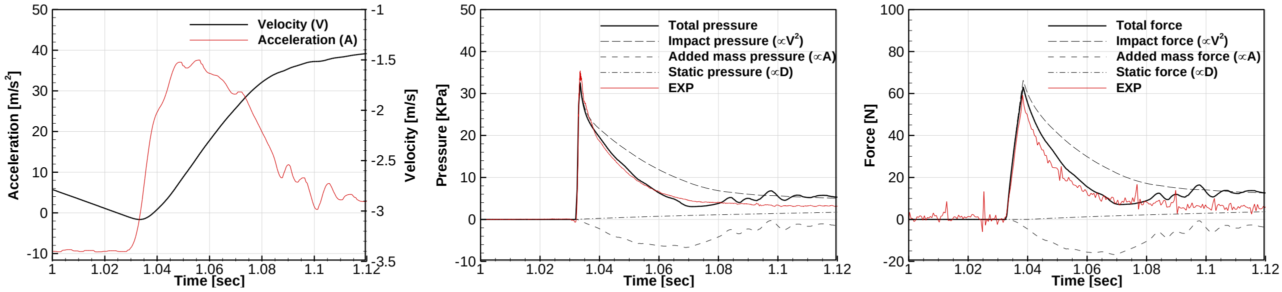

Fig. 2 Drop test of the wedge with a dead-rise angle of 30 degrees at a drop height of 0.5 m (left: falling velocity and acceleration, middle: pressure signals, right: force signals)

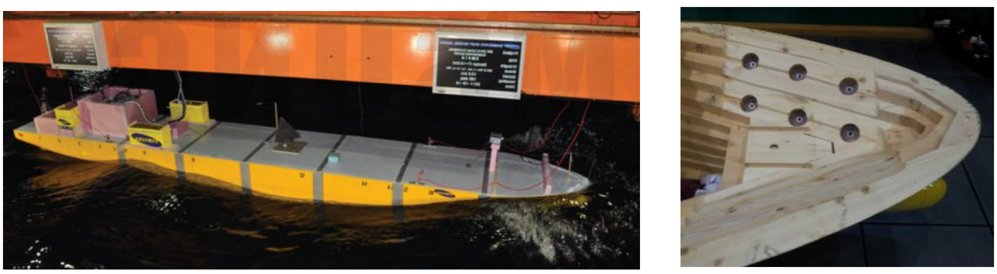

Fig.3 Model experiment for a 18,000TUE containership and installed pressure sensors at SSMB

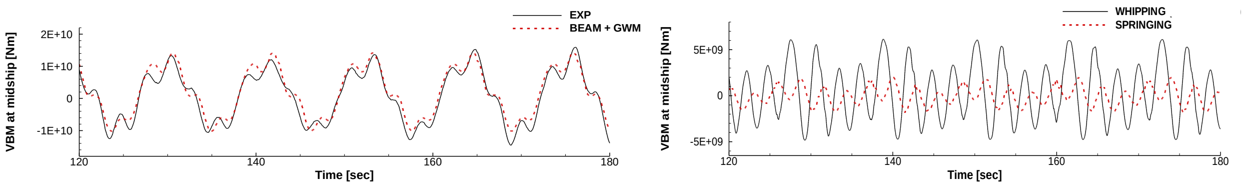

(a) Vertical bending moment at midship (b) Two components of hydroelasticity

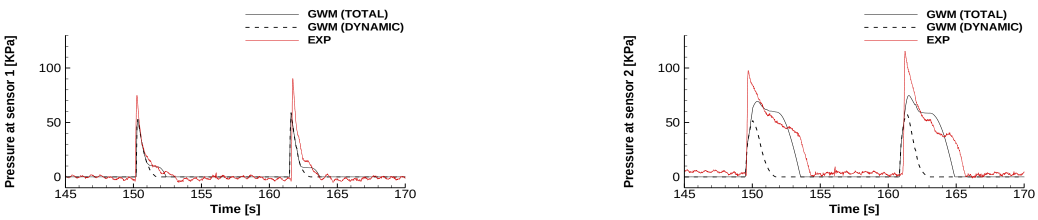

(c) Pressure at 10.5m above still water level (d) Pressure at 5.5m above still water level

Fig. 4 Comparison of vertical bending moments and slamming pressures in regular waves: wave height=12.2 m, wave period=14.0 sec, forward speed=10.0 knots